Tetrahedron Letters xxx (xxxx) xxx

Contents lists available at ScienceDirect

Tetrahedron Letters

journal homepage: www.elsevier.com/locate/tetlet

Control of enantioselectivity in the enzymatic reduction of halogenated acetophenone analogs by substituent positions and sizes

Afifa Ayu Koesoema [a], Daron M. Standley [b], Shusuke Ohshima [a], Mayumi Tamura [a], Tomoko Matsuda [a,*]

[a] Department of Life Science and Technology, School of Life Science and Technology, Tokyo Institute of Technology, 4259 Nagatsuta-cho Midori-ku, Yokohama 226-8501, Japan
[b] Department of Genome Informatics, Genome Information Research Center, Research Institute of Microbial Diseases, Osaka University, 3-1 Yamadaoka, Suita, Osaka 565-0871, Japan

ARTICLE INFO

Article history:
Received 31 January 2020
Revised 5 March 2020
Accepted 9 March 2020
Available online xxxx

Keywords:
Enantioselectivity control
Alcohol dehydrogenase
Asymmetric reduction
Halogenated acetophenone analogs

ABSTRACT

We utilized acetophenone reductase from *Geotrichum candidum* NBRC 4597 (*Gc*APRD), wild type and Trp288Ala mutant, to reduce halogenated acetophenone analogs to their corresponding (*S*)- and (*R*)-alcohols beneficial as pharmaceutical intermediates. Reduction by wild type resulted in excellent (*S*)-enantioselectivity for all of the substrates tested. Meanwhile, reduction by Trp288Ala resulted in high (*R*)-enantioselectivity for the reduction of 4′ substituted acetophenone and 2′-trifluoromethylacetophenone. In addition to that, we were able to control the enantioselectivity of Trp288Ala by the positions and sizes of the halogen substituents.

Introduction

Enantiomerically pure 1-phenylethanol analogs with halogen or halogenated group substituents (**2b**-**12b**) are versatile pharmaceutical intermediates [1]. For example, (*S*)-1-(3′,4′-dichlorophenyl) ethanol ((*S*)-**8b**) is an intermediate of sertraline, an obsessive-compulsive disorder medication [2,3]. Both (*S*)- and (*R*)-fluoro substituted 1-phenylethanol are potential intermediate of various bioactive compounds [4]. (*S*)-1-(2′-Fluorophenyl)ethanol ((*S*)-**2b**) is an intermediate of JN-403, a nicotinic acetylcholine receptor α7 agonist with therapeutic potential in a variety of neurological disorders [5]. (*S*)-1-(3′-Fluorophenyl)ethanol ((*S*)-**3b**) is an intermediate of EGFR and HER2 kinase inhibitors, a potential agent for cancer treatment [6]. (*R*)-1-(4′-Fluorophenyl)ethanol ((*S*)-**4b**) is an intermediate of anti-malaria drug [7], and gamma-secretase modulator useful for Alzheimer's disease treatment [8]. Trifluoromethyl substituted 1-phenylethanol such as (*R*)-1-(2′-trifluoromethylphenyl)ethanol ((*R*)-**12b**), being bulkier and more challenging to be synthesized, is needed as an intermediate of lysophosphatidic receptors' agonist for the treatment of pulmonary fibrosis [4].

Alcohol dehydrogenases (ADHs) [4,9,10] have been employed to reduce halogenated acetophenone analogs to produce the corresponding (*S*)-alcohols [11–13]. There are only a few (*R*)-selective ADHs existing in nature [14–16], although the (*R*)-alcohols are also needed as pharmaceutical intermediates. Thus, rational design [16–20] was employed on ADH to produce both (*S*)- and (*R*)-1-phenylethanol analogs. However, to the best of our knowledge, systematic and precise studies investigating the correlation between the halogen substituent positions and sizes with the enantioselectivity of an ADH have not been conducted.

Our group utilized the acetone powder (dried cell) of *Geotrichum candidum* NBRC 4597 (APG4), containing several (*S*)-ADHs and (*R*)-ADHs to reduce halogenated acetophenone analogs enantioselectively [12]. We have purified and overexpressed one of the (*S*)-ADH in APG4, *Geotrichum candidum* acetophenone reductase (*Gc*APRD) [21,22] and characterized it as a robust enzyme with excellent (*S*)-enantioselectivity in reducing unsubstituted acetophenone, 4-phenyl-2-butanone, various aliphatic ketones such as 2-butanone and 3-hexanone [23], as well as various cyclic ketones such as 2-tetralone and its analogs (5-MeO, 6-OH, 6-MeO, 6-Cl, and 7-MeO) [24]. Crystal structure of *Gc*APRD has been determined [23,25], and several rational mutational studies have been done to modify the Zn^{2+} coordination dynamics (Val153) [26], and to alter the substrate specificity as well as enantioselectivity (Trp288) [27]. Changing Trp288, located in the small binding pocket of *Gc*APRD, into smaller amino acid residue had enlarged the pocket.

In this study, we investigated the reduction of halogenated acetophenone analogs by *Gc*APRD wild type and Trp288Ala in detail (Fig 1). The wild type reduced all of the halogenated acetophenone analogs tested to their corresponding (*S*)-alcohols (*ee* >99%). Meanwhile, we could control Trp288Ala enantioselectivity based on the

* Corresponding author.
E-mail address: tmatsuda@bio.titech.ac.jp (T. Matsuda).

https://doi.org/10.1016/j.tetlet.2020.151820
0040-4039/

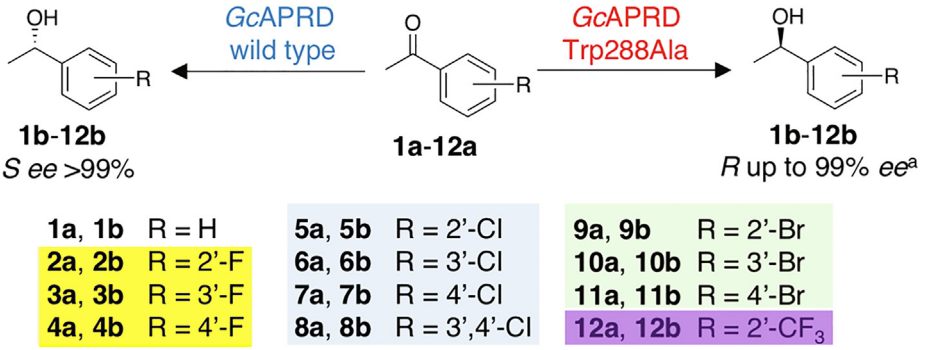

Fig. 1. Asymmetric reduction of halogenated acetophenone analogs by *Gc*APRD wild type and Trp288Ala. [a](*S*) of low *ee* for **1a** and **3a**. Fluoride, chloride, bromide, and trifluoromethyl substituents are indicated with yellow, blue, green, and purple background, respectively. (For interpretation of the references to colour in this figure legend, the reader is referred to the web version of this article.)

positions and sizes of halogen substituent in the phenyl ring. Enantioselectivity shifted from (*S*) to (*R*), and we obtained the highest (*R*)-enantioselectivity (*ee* up to 99%) for the reduction of 4′ substituted acetophenone and 2′-trifluoromethylacetophenone. *Gc*APRD wild type and Trp288Ala are useful catalysts to produce beneficial halogenated 1-phenylethanol analogs in (*S*)- and (*R*)-configuration.

Results and discussions

At first, kinetic studies (Michaelis-Menten constant (*K*m) and *k*cat determination) of *Gc*APRD wild type and Trp288Ala towards halogenated acetophenone analogs were conducted (Table S2) to assess the possibility of their preparative scale asymmetric reduction. For the wild type, the presence of substitution in the 2′ position (**2a**, **5a**, and **9a**) decreased the *K*m compared with **1a**. *K*cat (s^{-1}) values for the wild type were comparable with **1a**, or higher for some substrates (**8a, 10a**, and **11a**). We observed substrate inhibitions for halogenated acetophenone analogs with substitution in the 2′ and 3′ position, but not 4′ position, except **7a**.

Meanwhile, for Trp288Ala, the presence of substitution in the 2′ position (**2a**, **5a**, and **9a**) also decreased the *K*m compared with **1a**. Favorably, *k*cat (s^{-1}) values for halogenated substrates increased up to 15 times (**9a**) of that of **1a**. Substitution in the 2′ position (**2a**, **5a**, and **9a**) had much higher *k*cat than **1a** although it was the most sterically hindered. Halogen substituents in the 2′ position could induce polarization of the carbonyl group by the presence of concomitant orbital overlap between the carbonyl oxygen and halogen group, as observed in xylose reductase from *Candida tenuis* [28]. Substrate inhibition was only observed for Br substitution in the 2′ (**9a**) and 3′ (**10a**) positions. The kinetic parameters of the wild type and Trp288Ala were comparable to other ADHs for halogenated acetophenone analogs reduction [17,20]. With satisfactory kinetic parameters, we conducted the preparative scale asymmetric reduction. The results are shown in Fig. 2. For the wild type-catalyzed reduction of **1a**-**12a**, we employed 2-propanol as the cofactor regeneration system. The wild type-catalyzed reduction proceeded with satisfactory yield (Fig 2a) and excellent enantioselectivity in (*S*)-configuration (Fig 2c) independent of the positions and sizes of the halogen substituents. The reduction of sterically bulky 2′-trifluoromethylacetophenone (**12a**) also succeeded in giving the corresponding (*S*)-alcohol in 77% yield and >99% *ee*.

The yield may be affected more by the thermodynamic equilibrium position of the 2-propanol cofactor regeneration system rather than the kinetic parameters. The substrate concentration used in the reaction (~10 mM) was much higher than *K*m, and the reaction time was long enough to make the effect from *k*cat negligible. Although substitutions mainly in the 2′ and 3′ position (**2a**-**3a**, **5a**-**7a**, and **9a**-**10a**) displayed some substrate inhibition, the reduction still proceeded with satisfactory yield. No effect on positions and sizes of substituent on yield and enantioselectivity was also observed in the reduction by ADHs from *Saccharomyces cerevisiae* [29] and *Haloferax volcanii* [30].

For Trp288Ala-catalyzed reduction of **1a**-**12a**, we employed glucose/glucose dehydrogenase (GDH) as the cofactor regeneration system because the reactivity of Trp288Ala towards 2-propanol oxidation was poor. Trp288Ala-catalyzed reduction proceeded with a satisfactory yield (Fig 2b), and the yields did not relate to the *k*cat values and may be determined by the stability of Trp288Ala in the presence of various substrates. The equilibrium between oxidation–reduction is not related since the GDH shifted the equilibrium position from glucose towards gluconolactone. It was reported in the reduction by *Lactobacillus brevis* ADH that enzyme stability was one of the factors affecting yield in the asymmetric reduction of ketones [31,32].

The enantioselectivity of Trp288Ala-catalyzed reduction of substituted acetophenone analogs is mostly opposite from the wild type. Only a single mutation changed the enantioselectivity significantly. For Trp288Ala-catalyzed reduction, the presence of halogen substituents inverted the enantioselectivity from (*S*) for an unsubstituted substrate (**1a**) to (*R*) for substituted substrates (**2a**-**12a**, except for **3a**) (Fig. 2d). Substrates with substitutions in the 2′ position (**2a**, **5a**, and **9a**) were reduced with a moderate (*R*)-enantioselectivity. The enantioselectivity got higher in (*R*)-configuration when the substituent size was getting larger (*ee* (*R*): F < Cl < Br). Thus, we performed the reduction of **12a** with larger trifluoromethyl group in the 2′ position by Trp288Ala with the hope of obtaining even higher (*R*)-enantioselectivity. To our delight, the reduction proceeded with satisfactory yield and 99% *ee* (*R*), completely opposite from the enantioselectivity achieved by using the wild type. To the best of our knowledge, we were the first to report the enantioselective reduction of **12a** to the corresponding (*R*)-**12b** by using ADHs. As mentioned earlier, (*R*)-**12b** is an intermediate of pulmonary fibrosis drug [4].

Substrates with substitutions in the 3′ position (**3a**, **6a**, and **10a**) were reduced with (*S*)- or (*R*)-enantioselectivity depending on the size of the substituents. Substrate with F-substitution (**3a**) was reduced with (*S*)-enantioselectivity, Cl-substitution (**6a**) was reduced with moderate (*R*)-enantioselectivity, and Br-substitution (**10a**) was reduced with high (*R*)-enantioselectivity (*ee*: F (*S*), Cl (*R*) < Br (*R*)). Substrates with substitutions in the 4′ position (**4a**, **7a**, **8a**, and **11a**) were reduced with the highest (*R*)-enantioselectivity (92–96% *ee* (*R*)). It was clear that we were able to control the reduction enantioselectivity of Trp288Ala systematically based on the halogen substituent positions and sizes.

Please cite this article as: A. A. Koesoema, D. M. Standley, S. Ohshima et al., Control of enantioselectivity in the enzymatic reduction of halogenated acetophenone analogs by substituent positions and sizes, Tetrahedron Letters, https://doi.org/10.1016/j.tetlet.2020.151820

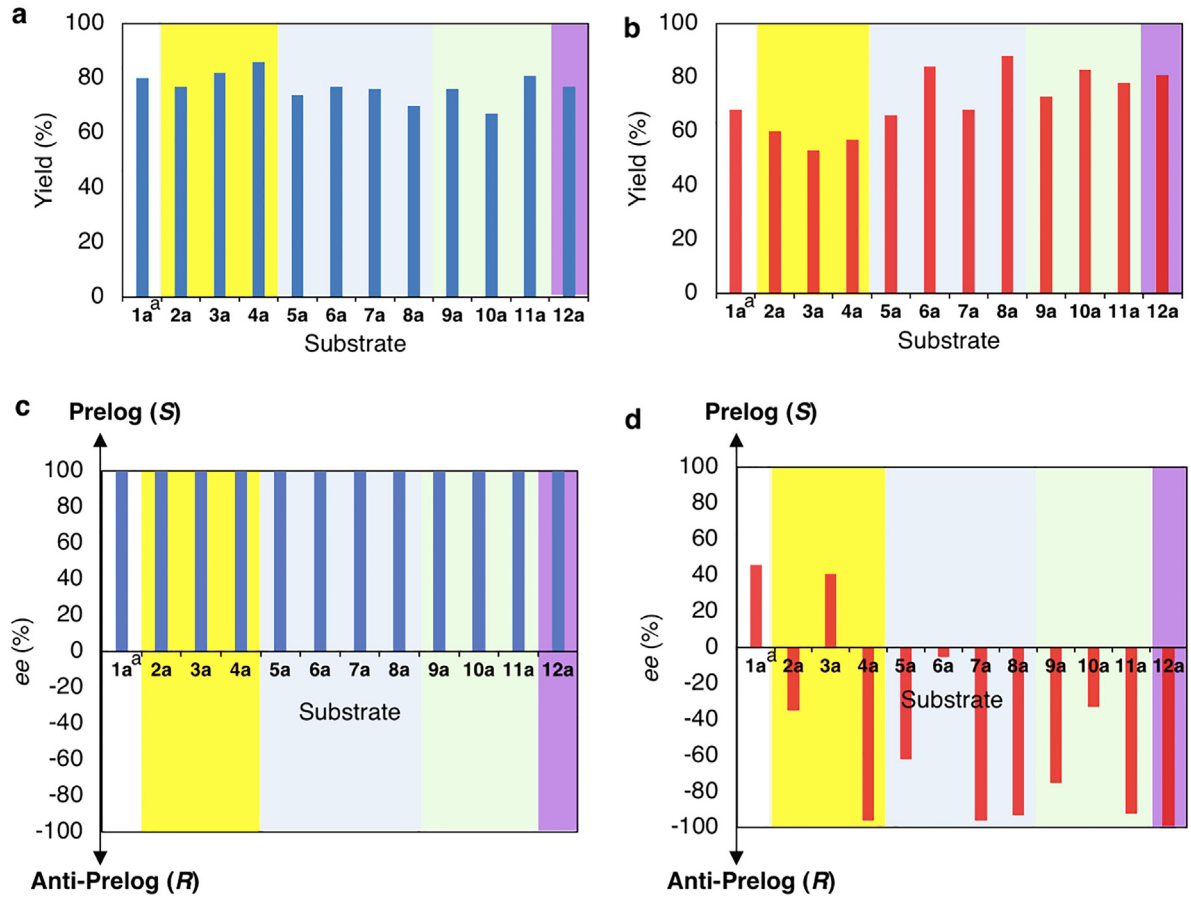

Fig. 2. Asymmetric reduction of halogenated acetophenone analogs (**1a**-**12a**) by *Gc*APRD wild type, and Trp288Ala. Isolated yield of reduction by **a** wild type, and **b** Trp288Ala. *ee* (%) of reduction by **c** wild type, and **d** Trp288Ala. Preparative scale reductions were done under the conditions described in supporting information. [a]Reaction yield and *ee* for reduction of **1a** by wild type and Trp288Ala was published previously [27]. Positive and negative *ee* values indicates Prelog (*S*) and anti-Prelog (*R*) enantiopreference, respectively. Fluoride, chloride, bromide, and trifluoromethyl substituents are indicated with yellow, blue, green, and purple background, respectively. (For interpretation of the references to colour in this figure legend, the reader is referred to the web version of this article.)

Reduction by other Trp288 mutants can give further insight into the binding configurations of halogenated acetophenone analogs. We employed three Trp288 mutants reported in our previous works [24,27]–Trp288Phe, Trp288Met, and Trp288Val–to reduce a representative substrate (**12a**). The *ee* values for Trp288Phe, Trp288Met, and Trp288Val were >99% (*S*), 50% (*S*), and 81% (*R*), respectively. As the size of the engineered pocket was increased, the enantioselectivity shifted from *S* to *R*. These results correlated with our previous observation that the size of the engineered pocket affects the reduction enantioselectivity [24,27].

We then tried to determine the cause of the enantioselectivity inversion of halogenated acetophenone analogs reduction by Trp288Ala. We hypothesized the presence of interaction between 4′-halogen substituent or 2′-trifluoromethyl substituents, for example 4′-Cl, with the engineered pocket of Trp288Ala, resulting in its very high (*R*)-enantioselectivity (Fig. S1a). Previously, by docking simulation, we found an interaction between the butyl group and the loop containing Gly94 in the engineered pocket of Trp288Ala [27], explaining the >99% *ee* (*S*) for 1-phenylpentan-1-one or butyl phenyl ketone reduction (Fig. S1b). To assess the presence of interaction between halogen substituent in the 4′ position and engineered pocket, we conducted the reduction of 1-(4′-chlorophenyl)-1-pentanone or butyl 4′-chlorophenyl ketone (**13a**) (Fig. S1c). The decrease of *ee* from >99% (*S*) in the reduction of unsubstituted butyl phenyl ketone to 74% (*S*) in the reduction of **13a** indicated the presence of some binding affinity between 4′ Cl substituent and the engineered pocket.

To examine our hypothesis, we performed docking simulations of the three representative substrates with high (*R*)-enantioselectivity **4a**, **7a**, and **12a** using the wild type crystal structure [23,25] and the Trp288Ala model structure [24] (Fig 3) with the addition of side chain flexibility as mentioned in supporting information. Because the Trp288Ala mutant did not readily crystalize, we modelled the Trp288Ala mutation on the wild type crystal structure, as described in supporting information. The binding energy values and details for the wild type and Trp288Ala can be seen in Table S3 and Table S4, respectively. Consistent with the experimental result, productive pro-(*S*) binding poses were found for the docking of **4a** (Fig. 3a), **7a** (Fig. 3c), and **12a** (Fig. 3e) in the active site of the wild type. In these binding poses, the halogen substituents of **4a**, **7a**, and **12a** may interact through van der Waals interactions with Leu264, while their methyl group interacted with either Leu122 or Trp288 in accordance with the previously reported interaction of methyl group in aliphatic ketones with Trp288 [23].

We found a productive pro-*R* binding pose for the docking of **4a** (Fig. 3b), **7a** (Fig. 3d), and **12a** (Fig. 3f) in the active site of the Trp288Ala. The fluorine substituent of **4a** and chlorine substituent of **7a** interacted through a C-X···hydrogen bond donor (C-X···HBD interaction) with the NH_2 group in the side chain of Asn119 in the engineered pocket, while the methyl substituent interacted with Leu264 in the large pocket. The distances between substrates' halogen substituents and C_δ of Asn119 (3.3 Å and 3.5 Å for **4a** and **7a**, respectively), as

Please cite this article as: A. A. Koesoema, D. M. Standley, S. Ohshima et al., Control of enantioselectivity in the enzymatic reduction of halogenated acetophenone analogs by substituent positions and sizes, Tetrahedron Letters, https://doi.org/10.1016/j.tetlet.2020.151820

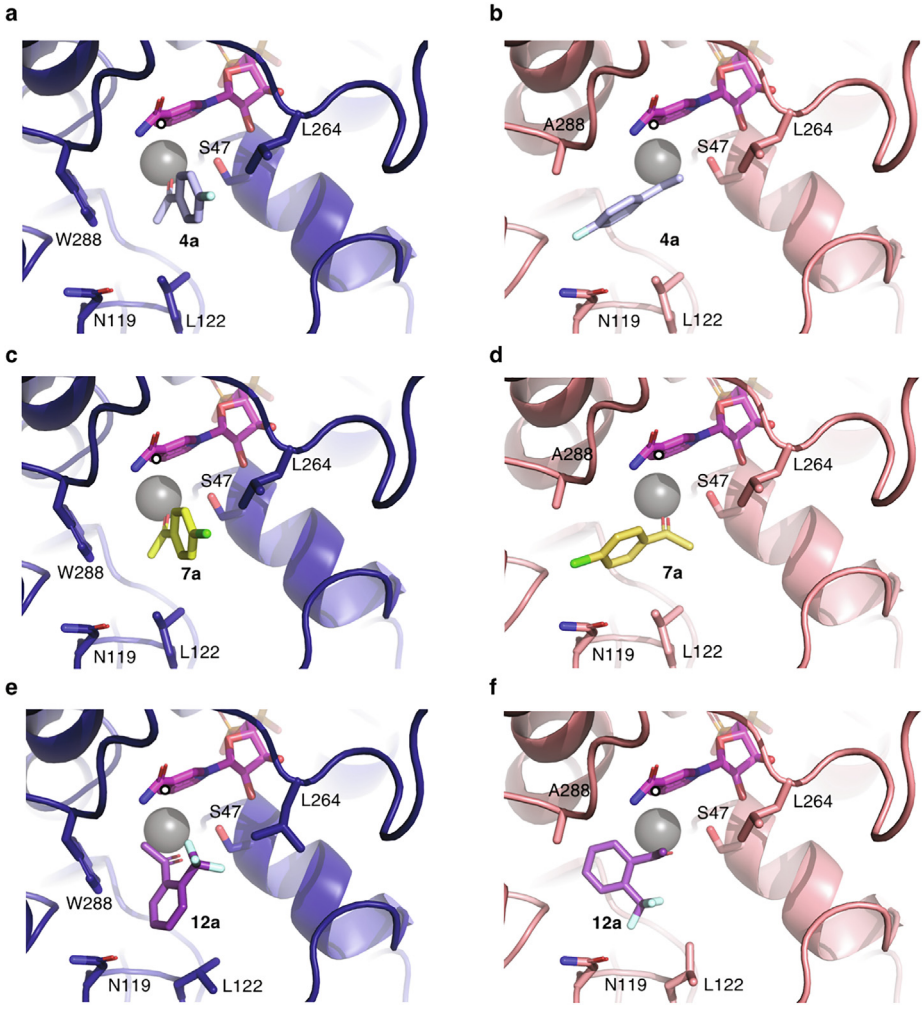

Fig. 3. Binding poses of **a 4a** in the active site of *Gc*APRD wild type crystal structure, **b 4a** in the active site of *Gc*APRD Trp288Ala model structure, **c 7a** in the active site of *Gc*APRD wild type crystal structure, **d 7a** in the active site of *Gc*APRD Trp288Ala model structure, **e 12a** in the active site of *Gc*APRD wild type crystal structure, and **f 12a** in the active site of *Gc*APRD Trp288Ala model structure. The CPK coloring was used except for the backbone of the receptor. NADH are shown in purple stick. Catalytic zinc is shown in grey sphere, and the C4 of NADH with hydride to be transferred to the ketone is highlighted with white circle. (For interpretation of the references to colour in this figure legend, the reader is referred to the web version of this article.)

well as C-X···HBD angle (133° and 110° for **4a** and **7a**, respectively), were among the average of other reported crystal structures in PDB containing halogenated ligands with C-X···HBD interaction [33]. For **12a**, the pro-*R* binding pose was stabilized through a van der Waals interaction of the trifluoromethyl substituent with Asn119 and Leu122 in the engineered pocket of Trp288Ala.

In addition, we performed docking simulations of 2′ (**2a** and **5a**) and 3′ (**3a** and **6a**) substituted acetophenones with low (*R*)-enantioselectivity (except **3a**) in the model structure of Trp288Ala, with the addition of side chain flexibility to Leu122 or Phe287, following the same protocol used for 4′-substituted acetophenones (Fig. S2 and Table S5, detailed discussions can be found in supporting information). The crucial C-X···HBD interaction with Asn119, found in 4′ substituted acetophenone (Fig. 3b and d), could not be formed in the docking poses of 2′ and 3′ substituted acetophenone, which may result in their low (*R*)-enantioselectivities. Altogether the docking simulations have supported the importance of interactions with the halogen substituents or trifluoromethyl group with the amino acids in the engineered pocket for the high (*R*)-enantioselectivity observed in the reduction of **4a**, **7a**, and **12a**.

Conclusions

By the utilization of *Gc*APRD wild type and Trp288Ala, we could enantioselectively reduce the halogenated acetophenone analogs to their corresponding (*S*)- and (*R*)-alcohols, pharmaceutically important intermediates. Importantly, sterically bulky (*S*) and (*R*)-**12b** were synthesized in >99% *ee* (*S*) and 99% (*R*) by the wild type and Trp288Ala, respectively. We were able to clearly and systematically control the reduction enantioselectivity based on the positions and sizes of halogen substituents in the phenyl ring for the reduction by Trp288Ala.

Declaration of Competing Interest

The authors declare that they have no known competing financial interests or personal relationships that could have appeared to influence the work reported in this paper.

Acknowledgments

The authors acknowledged Professor Miki Senda and Professor Toshiya Senda from High Energy Accelerator Research Organiza-

Please cite this article as: A. A. Koesoema, D. M. Standley, S. Ohshima et al., Control of enantioselectivity in the enzymatic reduction of halogenated acetophenone analogs by substituent positions and sizes, Tetrahedron Letters, https://doi.org/10.1016/j.tetlet.2020.151820

tion (KEK), Japan, for the help with the crystallization of enzymes and valuable discussions. This work was supported by the Japan Society for the Promotion of Science, Japan (grant number JP16K05864) to Tomoko Matsuda and the Platform Project for Supporting Drug Discovery and Life Science Research (Basis for Supporting Innovative Drug Discovery and Life Science Research (BINDS)) from AMED, Japan (grant number 19am0101108j0003) to Daron M. Standley.

Appendix A. Supplementary data

Supplementary data to this article can be found online at https://doi.org/10.1016/j.tetlet.2020.151820.

References

[1] M.L. Contente, I. Serra, L. Palazzolo, C. Parravicini, E. Gianazza, I. Eberini, A. Pinto, B. Guidi, F. Molinari, D. Romano, Org. Biomol. Chem. (2016) 3404–3408, https://doi.org/10.1039/c6ob00047a.
[2] H. Liu, B.S. Chen, F.Z. Ribeiro de Souza, L. Liu, Mar. Drugs. 16 (2018) 62, https://doi.org/10.3390/md16020062.
[3] C. Barbieri, E. Caruso, P. D'Arrigo, G. Pedrocchi Fantoni, S. Servi, Tetrahedron Asymmetry 10 (1999) 3931–3937, https://doi.org/10.1016/S0957-4166(99)00402-4.
[4] B.H. Hoff, E. Sundby, Bioorg. Chem. 51 (2013) 31–47, https://doi.org/10.1016/j.bioorg.2013.09.003.
[5] D. Feuerbach, J. Nozulak, K. Lingenhoehl, K. McAllister, D. Hoyer, Neurosci. Lett. 416 (2007) 61–65, https://doi.org/10.1016/j.neulet.2007.01.045.
[6] H. Mastalerz, M. Chang, P. Chen, P. Dextraze, B.E. Fink, A. Gavai, B. Goyal, W.C. Han, W. Johnson, D. Langley, F.Y. Lee, P. Marathe, A. Mathur, S. Oppenheimer, E. Ruediger, J. Tarrant, J.S. Tokarski, G.D. Vite, D.M. Vyas, H. Wong, T.W. Wong, H. Zhang, G. Zhang, Bioorganic Med. Chem. Lett. 17 (2007) 2036–2042, https://doi.org/10.1016/j.bmcl.2007.01.002.
[7] F.J.B. Cardoso, A.F. de Figueiredo, M. da Silva Lobato, R.M. de Miranda, R.C.O. de Almeida, J.C. Pinheiro, J. Mol. Model. 14 (2008) 39–48, https://doi.org/10.1007/s00894-007-0249-9.
[8] X. Huang, R. Aslanian, W. Zhou, X. Zhu, J. Qin, W. Greenlee, Z. Zhu, L. Zhang, L. Hyde, I. Chu, M. Cohen-Williams, A. Palani, ACS Med. Chem. Lett. 1 (2010) 184–187, https://doi.org/10.1021/ml1000799.
[9] K. Rosenthal, S. Lütz, Curr. Opin. Green Sustain. Chem. 11 (2018) 58–64, https://doi.org/10.1016/j.cogsc.2018.03.015.
[10] M.M. Musa, R.S. Phillips, Catal. Sci. Technol. 1 (2011) 1311–1323, https://doi.org/10.1039/c1cy00160d.
[11] D. Zhu, H.T. Malik, L. Hua, Tetrahedron Asymmetry 17 (2006) 3010–3014, https://doi.org/10.1016/j.tetasy.2006.10.042.
[12] K. Nakamura, T. Matsuda, J. Org. Chem. 63 (1998) 8957–8964, https://doi.org/10.1021/jo9812779.
[13] D. Zhu, B.E. Rios, J.D. Rozzell, L. Hua, Tetrahedron Asymmetry. 16 (2005) 1541–1546, https://doi.org/10.1016/j.tetasy.2005.02.030.
[14] D. Zhu, Y. Yang, L. Hua, J. Org. Chem. 71 (2006) 4202–4205, https://doi.org/10.1021/jo0603328.
[15] N. Itoh, Appl. Microbiol. Biotechnol. 98 (2014) 3889–3904, https://doi.org/10.1007/s00253-014-5619-5.
[16] D. Zhu, Y. Yang, S. Majkowicz, T.H.-Y. Pan, K. Kantardjieff, L. Hua, Org. Lett. 10 (2008) 525–528, https://doi.org/10.1021/ol702638j.
[17] C.M. Nealon, T.P. Welsh, C.S. Kim, R.S. Phillips, Arch. Biochem. Biophys. 606 (2016) 151–156, https://doi.org/10.1016/j.abb.2016.08.002.
[18] Y. Nie, S. Wang, Y. Xu, S. Luo, Y.-L. Zhao, R. Xiao, G.T. Montelione, J.F. Hunt, T. Szyperski, ACS Catal. 8 (2018) 5145–5152, https://doi.org/10.1021/acscatal.8b00364.
[19] S. Wang, Y. Nie, Y. Xu, R. Zhang, T.-P. Ko, C.-H. Huang, H.-C. Chan, R.-T. Guo, R. Xiao, Chem. Commun. 50 (2014) 7770–7772, https://doi.org/10.1039/c4cc01752h.
[20] H. Li, Y. Yang, D. Zhu, L. Hua, K. Kantardjieff, J. Org. Chem. 75 (2010) 7559–7564, https://doi.org/10.1021/jo101541n.
[21] Y. Nakata, T. Fukae, R. Kanamori, S. Kanamaru, T. Matsuda, Appl. Microbiol. Biotechnol. 86 (2010) 625–631, https://doi.org/10.1007/s00253-009-2329-5.
[22] T. Yamamoto, Y. Nakata, C. Cao, Y. Sugiyama, Y. Asanuma, S. Kanamaru, T. Matsuda, Appl. Microbiol. Biotechnol. 97 (2013) 10413–10421, https://doi.org/10.1007/s00253-013-4801-5.
[23] A.A. Koesoema, Y. Sugiyama, Z. Xu, D.M. Standley, M. Senda, T. Senda, T. Matsuda, Appl. Microbiol. Biotechnol. 103 (2019) 9543–9553, https://doi.org/10.1007/s00253-019-10093-w.
[24] A.A. Koesoema, D.M. Standley, K. T.sriwong, M. Tamura, T. Matsuda, Tetrahedron Lett. 61 (13) (2020) 151682, https://doi.org/10.1016/j.tetlet.2020.151682.
[25] Y. Sugiyama, M. Senda, T. Senda, T. Matsuda, Acta Crystallogr. Sect. F 71 (2015) 320–323, https://doi.org/10.1107/S2053230X15002265.
[26] D. Schritt, K. Katoh, S. Li, D.M. Standley, Future Directions in Biocatalysis, second ed., 2017: pp. 385–398.
[27] A.A. Koesoema, Y. Sugiyama, K. T.sriwong, Z. Xu, S. Verina, D.M. Standley, M. Senda, T. Senda, T. Matsuda, Appl. Microbiol. Biotechnol. 103 (2019) 9529–9541, https://doi.org/10.1007/s00253-019-10206-5.
[28] M. Vogl, R. Kratzer, L. Brecker, Org. Biomol. Chem. 9 (2011) 5863, https://doi.org/10.1039/c1ob05510k.
[29] Y. Yang, D. Zhu, T.J. Piegat, L. Hua, Tetrahedron Asymmetry. 18 (2007) 1799–1803, https://doi.org/10.1016/j.tetasy.2007.08.008.
[30] D. Alsafadi, S. Alsalman, F. Paradisi, Org. Biomol. Chem. 15 (2017) 9169–9175, https://doi.org/10.1039/c7ob02299a.
[31] F.R. Bisogno, E. García-Urdiales, H. Valdés, I. Lavandera, W. Kroutil, D. Suárez, V. Gotor, Chem. - A Eur. J. 16 (2010) 11012–11019, https://doi.org/10.1002/chem.201001233.
[32] C. Rodríguez, W. Borzęcka, J.H. Sattler, W. Kroutil, I. Lavandera, V. Gotor, Org. Biomol. Chem. 12 (2014) 673–681, https://doi.org/10.1039/c3ob42057d.
[33] F.Y. Lin, A.D. Mackerell, J. Phys. Chem. B. 121 (2017) 6813–6821, https://doi.org/10.1021/acs.jpcb.7b04198.

Please cite this article as: A. A. Koesoema, D. M. Standley, S. Ohshima et al., Control of enantioselectivity in the enzymatic reduction of halogenated acetophenone analogs by substituent positions and sizes, Tetrahedron Letters, https://doi.org/10.1016/j.tetlet.2020.151820